Immunity, Vol. 9, 135–141, July, 1998, Copyright ©1998 by Cell Press

Hot Spot Focusing of Somatic Hypermutation in MSH2-Deficient Mice Suggests Two Stages of Mutational Targeting

Cristina Rada,† Michael R. Ehrenstein,† Michael S. Neuberger,* and César Milstein
Medical Research Council Laboratory of Molecular Biology
Hills Road
Cambridge CB2 2QH
United Kingdom

Summary

Likely creation of mismatches during somatic hypermutation has stimulated interest in the effect of mismatch repair deficiency on the process. Analysis of unselected mutations in the 3′ flank of V_H rearrangements in germinal center B cells revealed that MSH2 deficiency caused a 5-fold reduced mutation accumulation. This might reflect ectopic effects of the *Msh2* disruption; indeed, the mice exhibit other perturbations within the B cell compartment. However, that MSH2 (or factors dependent upon it) plays a role in the mechanism of mutation fixation is indicated by a strikingly increased focusing of the mutations on intrinsic hot spots. We propose two phases to hypermutation targeting. The first is hot spot focused and MSH2 independent; the second, MSH2-dependent phase yields a more even spread of mutation fixation.

Introduction

Somatic hypermutation of immunoglobulin V genes plays a central role in antibody diversification and affinity maturation (for reviews see Rajewsky, 1996; Storb, 1996; Weill, 1996; Parham, 1998). Multiple single-nucleotide substitutions are incorporated into a roughly 2 kb domain that includes the DNA that encodes the V region of the expressed antibody. The molecular mechanism of the process is not known, but most models envisage an involvement of error-prone DNA synthesis that will likely lead to a nucleotide mismatch between the newly synthesized, mutated DNA strand and its template partner. Were such a mismatch corrected in the conventional manner with the newly synthesized strand being repaired, one might envisage that the nucleotide substitutions created by the hypermutation process would be reverted to germline and that the intended effect of immunoglobulin V gene diversification thereby abrogated.

Several solutions to this conundrum can be envisioned. Mismatch repair in hypermutating B cells could be suppressed either globally or even locally (i.e., within the vicinity of the V gene segment). Alternatively, if hypermutation occured, say, during G1 with mismatch repair being restricted to late in S or G2, the mutations could be fixed by chromosome replication before mismatch repair became operative. Mechanisms have also been envisaged in which the mismatch repair process no longer relies exclusively on the parental DNA strand for templating its repair activity.

With such considerations in mind, one might expect the frequency of somatic hypermutation to be either unaffected or enhanced in mismatch repair–deficient mice. Several groups have now investigated this issue. The first report, from Cascalho et al. (1998), strikingly reported that the extent of V gene mutation in a putative memory B cell population of mice carrying a targeted V_H gene integration was considerably reduced when analyzed in mice deficient in PMS2 (a mammalian homolog of *E. coli mutL*). This led these authors to propose that in hypermutating B cells mismatch repair actually "corrects" nucleotide substitutions in the immunoglobulin loci according to the newly synthesized (as opposed to parental) DNA strand and therefore fixes the mutations rather than eliminates them. However, analyzing an antigen-specific response in immunized PMS2-deficient mice, Winter et al. (1998) did not observe such a profound reduction in mutation accumulation but rather noted an increase in adjacent nucleotide substitutions.

With regard to mice lacking MSH2 (a mammalian homolog of *mutS*), both Phung et al. (1998) and Jacobs et al. (1998) detected no major effect on the mutation frequency of V gene segments but did note an increased proportion of mutations occurring at Gs and Cs. In this work, we have also analyzed hypermutation in MSH2-deficient mice but, in this case, by looking at the accumulation and distribution of the unselected mutations in the intronic 3′ flank of V_H segments amplified from Peyer's patch germinal center B cells. Unlike Jacobs et al. (1998) and Phung et al. (1998), we observe considerably diminished mutation accumulation in MSH2-deficient mice. In addition, the altered mutational targeting is revealed as a striking focusing toward intrinsic hot spots. Since the most dominant intrinsic hot spots are at G/C, this hot spot focusing is consistent with the G/C bias noted by both these groups and discussed by Phung et al. (1998). However, the finding of hot spot focusing in combination with the diminished mutation accumulation gives alternative insights into the implication of the findings for models of antibody hypermutation.

Results

Diminished Mutation Accumulation

To analyze immunoglobulin gene hypermutation in MSH2-deficient mice, we used the strategy that we previously described to examine hypermutation in p53-deficient animals (Jolly et al., 1997). This strategy exploits the findings that (1) hypermutation is an ongoing process in the germinal centers of mouse Peyer's patches, since these cells are continuously responding to gut antigens (González-Fernández and Milstein, 1993); and (2) the mutation domain in the IgH locus extends downstream

* To whom correspondence should be addressed (e-mail: msn@mrc-lmb.cam.ac.uk).
† These authors contributed equally to this work.

Table 1. Mutation Frequency in Peyer's Patch Germinal Center B Cells

	Clones Analyzed			Mutation Frequency ($\times 10^{-3}$)	
	Total Number	Number Mutated	Total Number of Mutations	Calculated on the Basis of All Clones	Mutated Clones
Msh2$^{-/-}$	121	81	164	3.36	5.0
Msh2$^{+/-}$	95	71	739	19.3	25.8

of the productively rearranged J_H segment, well into the J_H-C_H intron (Lebecque and Gearhart, 1990). This means that mutation accumulation can readily be analyzed following PCR amplification of the J_H flanking region without need for specific immunization or for introduction of a marked transgene substrate. Furthermore, the fact that only mutations in the J_H-C_H intron are analyzed means that the deduced mutation pattern gives information about the instrinsic features of the mutational process without the severe skewing effects of specific antigen selection.

Peyer's patch germinal center B cells were obtained by cell sorting from litter-matched *Msh2*$^{-/-}$ and *Msh2*$^{+/-}$ mice. The J_H flanking region was PCR amplified using one oligonucleotide that primes forward from within framework 3 of the members of the abundantly used V_HJ558 family and a second oligonucleotide that primes backward from a site 1.2 kb downstream of J_H4. Since the resultant products span the V_HDHJ_H junction, clonal relatedness of amplified products could readily be identified.

Mice from two sets of litters were analyzed, and the assembled results reveal a roughly 5-fold reduction in mutation accumulation in the MSH2-deficient animals (Table 1). Despite variation between individuals, it is notable that this reduction is not so much a consequence of the fact that fewer germinal center B cells have undergone hypermutation at all, but rather that the bulk of cells have accumulated fewer mutations (Figure 1A). Thus, most of the cells carry at least one mutation, but there is a general shift toward a lower number of accumulated mutations in individual mutated cells. This is reminiscent of the pattern of mutation in young mice (González-Fernández et al., 1994a) and is consistent with the idea that germinal center B cells in MSH2-deficient mice undergo fewer rounds of hypermutation. Other explanations can also be envisaged.

Increased Focusing of Mutation on Intrinsic Hot Spots

When the distribution of mutations along the J_H flank is compared in normal and MSH2-deficient mice, a striking difference emerges (Figure 1C). Compared to their littermate controls, a large proportion of the nucleotide substitutions in the *Msh2*$^{-/-}$ database are found to be focused on a small number of positions. These positions reflect intrinsic mutational hot spots (Betz et al., 1993; Jolly et al., 1997) whose sequences conform well to the RGYW (R, purine; Y, pyrimidine; W, A/T) consensus of Rogozin and Kolchanov (1992), and this increased hot spot targeting is a feature of all three MSH2-deficient mice analyzed (Table 2). It is difficult to see how this hot spot targeting could simply be a consequence of the diminished mutation accumulation in Peyer's patches; increased focusing on hot spots is not a feature of hypermutation in young, wild-type mice, although such animals do show diminished mutation accumulation (legend to Table 2; unpublished data).

When the nucleotide substitution preferences of the mutations in the *Msh2*$^{-/-}$ and *Msh2*$^{+/-}$ mice are compared (Table 3), a marked alteration in the targeting pattern is observed. In *Msh2*$^{+/-}$ heterozygotes (as in wild-type mice), A residues are most frequently mutated. However, in the *Msh2*$^{-/-}$ littermates, there is a clear preference for mutations at G and less markedly at C, similar to what has been noted by Phung et al. (1998) and Jacobs et al. (1998). This discrepancy between a marked G preference in MSH2-deficient mice and an A-preference in wild-type animals is not solely apparent owing to increased mutation at the major hot spots (which, in the region analyzed, are themselves at G/C residues), since the discrepancy is even evident when the major hot spots are excluded from the analysis (Table 3).

Altered B Cell Subpopulations and Immune Responses

Thus, the data reveal that in the absence of MSH2 there is both dimished accumulation and altered targeting of somatic hypermutation, suggesting a role for the mismatch repair system in the molecular mechanism of mutation creation/fixation during somatic hypermutation. However, the results do not preclude a possible impact on the accumulation of mutations by more distant cellular disruptions caused by the MSH2 deficiency. We therefore analyzed aspects of B cell maturation and function in *Msh2*$^{-/-}$ mice to see if there were signs of immune system dysfunction that could not simply be ascribed to impaired hypermutation.

The germinal centers of spleens in MSH2-deficient mice were normal in size and appearance (Figure 2A), and indeed the proportion of Peyer's patch B cells staining brightly with fluoresceinated peanut agglutinin was similar to that in controls (data not shown). However, development of the specific immune response was impaired. Following secondary immunization with NP-CG, the titre of good-affinity IgG1 anti-NP antibody (as judged by ELISA titration on $NP_{2.5}$-BSA coated plates) was diminished—a phenomonenon which could conceivably be ascribable to impaired hypermutation (Figure 3A). But even at day 8 and 12 following primary immunization, we found a substantially diminished serum titre of IgG1 (but not IgM) anti-NP antibody (as judged by ELISA on NP_{30}-BSA-coated plates so as to detect low-affinity antibody [Figure 3B]).

No gross effects on proliferative responses of MSH2-deficient splenic B cells in these animals were detected

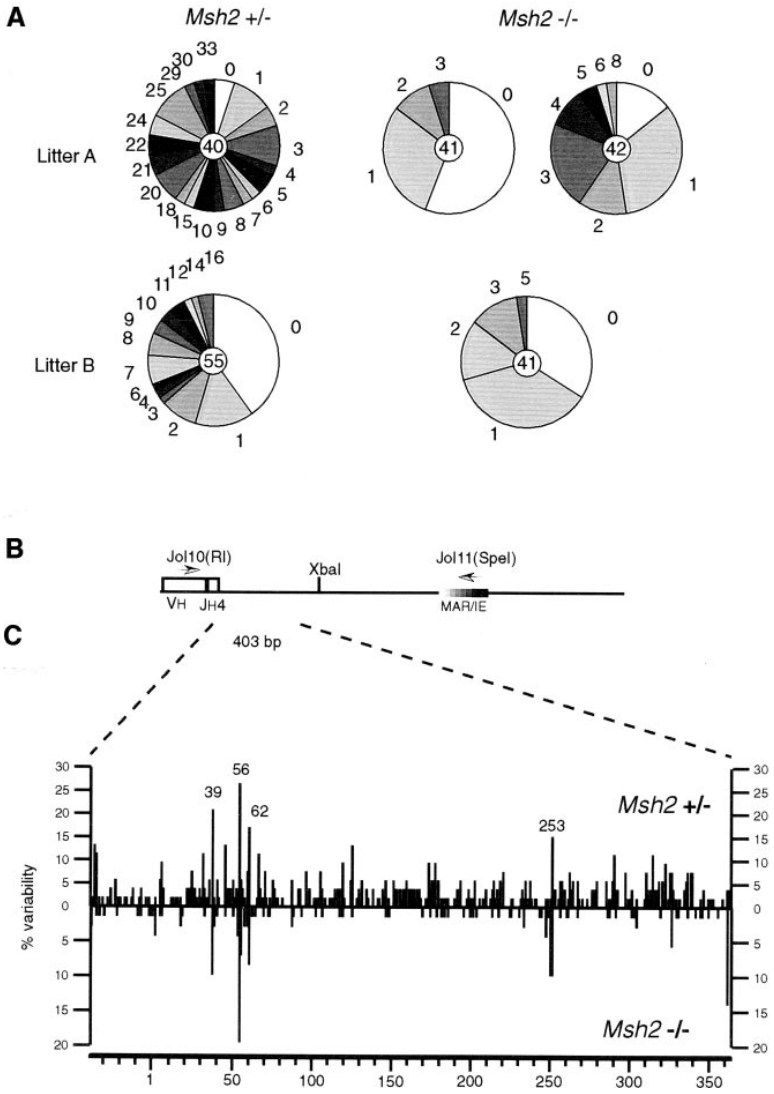

Figure 1. Analysis of Hypermutation

(A) Distribution of mutations in Peyer's patches germinal center B cells from *Msh2*$^{-/-}$ and *Msh2*$^{+/-}$ mice. Results are presented from two sets of litters. Litter A was 14 weeks old and spent its last 3 weeks housed in a conventional animal facility; litter B was 5 weeks old. The area of each sector in the pie charts represents the proportion of clones with the indicated number of mutations; the total number of clones analyzed is indicated in the central circle of each pie.

(B) Schematic representation of the segment of the J_H4-Cμ intron analyzed for mutations. For PCR amplification, a consensus primer in the framework 3 of the V_HJ558 family was used together with a primer in the IgH-intron enhancer.

(C) Mutation patterns in endogenous J_H4 flanking sequence of *Msh2*$^{+/-}$ (above the zero line) and *Msh2*$^{-/-}$ (below the zero line) mice. Variability (given as the percentage of clones with a mutation at that position) is given for each nucleotide position, with position +1 being the first nucleotide of the J_H4-Cμ intron. The major hot spots are indicated by their nucleotide position numbers.

(Figure 3C). This parallels observations made with non-lymphoid cells in the same line of mice (de Wind et al., 1995). However, we did observe consistent changes in B cell subpopulations. Thus, the IgM$^+$, IgD$^+$ splenic B cells of MSH2-deficient mice showed a shift toward increased surface IgM expression—typically taken as a sign of decreased maturity (Figure 2B). Also striking was the fact that in the bone marrow there was a marked diminution in the proportion of IgM$^+$, IgD$^+$, CD45R (B220)^{high} B cells, which are clasically identified as mature recirculating B cells (Figure 2C). Thus, there are some clear differences between the B cells and B cell responses of MSH2-deficient and control mice that are difficult to ascribe directly to impaired hypermutation.

Discussion

The work described here reveals that MSH2-deficient mice exhibit impaired mutation accumulation and increased focusing of the residual mutations on the intrinsic hot spots; the mice also exhibit significant changes in B cell subpopulations and immune responses. We consider here how these findings relate to observations made by others on hypermutation in mismatch repair–deficient mice and what insight the results give to the possible involvement of mismatch repair in the creation/fixation of nucleotide substitutions during antibody hypermutation.

Mutation Accumulation

Our finding of a substantially diminished level of hypermutation does not parallel the results of Phung et al. (1998) and Jacobs et al. (1998), who found little effect of *Msh2* disruption on the mutation frequency in MSH2-deficient mice. However, the diminished mutation frequency that we see is very similar to that first reported by Cascalho et al. (1998) for PMS2-deficient mice. We believe the explanation for the discrepancy lies in the method of analysis. In the approach used here (and probaly in that of Cascalho et al. [1998]), one is essentially taking a snapshot view of the frequency of mutations in the responses to diverse antigens, with these responses presumably being at various stages of maturation. Here we see reduced frequency of mutation.

Table 2. Distribution of Mutations in Hot Spots versus Background

Position		Mutations	
		Msh2$^{+/-}$	*Msh*$^{-/-}$
39	TGT	2.1% (11)	4.6% (7)
56	AGC	2.7% (14)	9.3% (14)
62	GCA	1.8% (9)	4.6% (7)
253	GCT	1.6% (8)	6.6% (10)
		8.2% (42)	25.1% (38)

Mutations at each hotspot are given as the percentage of total mutations that are located at that hot spot; the absolute number of such mutations in the database is provided in parentheses. Hot spots are defined here as nucleotide positions at which 15% of the sequences from *Msh2*$^{+/-}$ mice carry a mutation. No significant difference in the proportion of the total mutations located in the four major hot spots indicated was apparent when the control mice (5 and 14 weeks of age) were analyzed separately (6.7% and 9.1% of the mutations found in the hot spots). Furthermore, all three *Msh2*$^{+/-}$ mice, when analyzed individually, revealed a preferential accumulation of mutations in the four hot spots as compared to the controls.

Table 3. Nucleotide Targeting Comparison

	Msh2$^{-/-}$	*Msh2*$^{+/-}$	Compilation Database	Excluding Hot Spots	
				Msh2$^{-/-}$	Msh2$^{+/-}$
T	7%	18%	20%	10%	20%
C	30%	26%	23%	20%	23%
A	19%	34%	33%	27%	38%
G	43%	22%	24%	44%	19%

The table gives the percentage of the total mutations in each database that have occurred in each of the four bases as analyzed on the coding strand. The compilation database (which is formed from V gene, non–V gene, and V gene–flanking mutations, totaling 2803 mutations in >0.19 Mb of total DNA target analyzed) is taken from Milstein et al. (1998).

However, if, as in Phung et al. (1998), one looks at the number of mutations in antigen-selected hybridomas derived during the secondary response to a specific antigen, then it may well be that those cells that have survived the specific selection criteria do not show such a marked reduction in mutation.

A reduced overall mutation frequency could, in principle, be due to a decreased proportion of cells having undergone the hypermutation process at all or to a diminished extent of mutation accumulation in those cells within the otherwise normally targeted mutated population. Our results favor the second interpretation. This is particularly illustrated by the analysis of young mice where the proportion of unmutated cells is similar in *Msh2*$^{+/-}$ and *Msh2*$^{-/-}$ littermates; the difference lies in the number of mutations accumulated within the mutated cell population. A reduced accumulation of mutations in the targeted cells could then be due to a decreased number of mutations incorporated in each cycle of mutation or to a decreased number of cycles. The two cases could prove fundamentally different since one likely addresses the mechanics of hypermutation, the other, the cellular kinetics.

A reduced extent of mutation accumulation in mismatch repair–deficient mice could therefore, as first suggested by Cascalho et al. (1998), indicate a role for mismatch repair in the hypermutation process itself. However, PMS2 and MSH2 deficiency affects multiple aspects of biology. For example, the *Msh2*$^{-/-}$ mice develop T cell tumors at young age (de Wind et al., 1995) and, as shown here, they have a reduced number of recirculating B cells in bone marrow, with their splenic B cells shifted to increased IgM expression. Immune responses are also affected. Thus, while reduced mutation accumulation could reflect a role for mismatch repair in mutation, it could equally reflect ectopic effects such as increased DNA damage or decreased T cell help causing germinal center B cells to undergo fewer rounds of hypermutation. However, the altered pattern of mutational targeting in MSH2-deficient mice strongly suggests a role for MSH2 in the mechanics of mutation creation/fixation during hypermutation. Thus, taken together, it could well be that the diminished mutation frequency in MSH2-deficient mice reflects both altered mechanics of hypermutation and altered cellular dynamics.

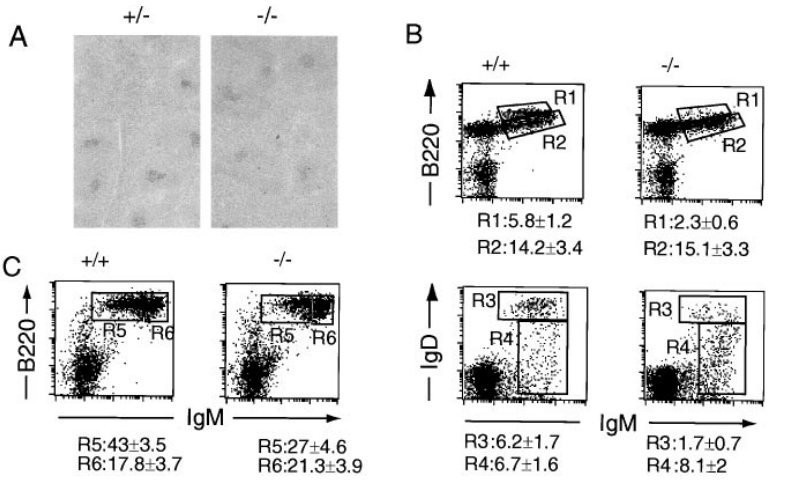

Figure 2. B Cell Populations

(A) Histological analysis to detect germinal centers (GCs) was performed on splenic sections of MSH2-deficient and control littermates prepared 14 days after immunization with NP-CG. GCs were revealed by staining with biotinylated peanut agglutinin. No difference in GC size or number was detected when comparing immunized MSH2-deficient mice to the immunized controls.

(B) Flow cytometric analysis of bone marrow cells stained with FITC-conjugated anti-mouse IgM and either PE-conjugated anti-IgD or PE-conjugated RA3-6B2 anti-CD45R (B220) MAb. Mature, recirculating B cells have an IgM^{+}, IgD^{+}, CD45R(B220)^{high} phenotype and would be expected to be found in areas R1 and R3. The profiles shown are representative of six mice analyzed, and the mean percentage of cells (± SEM) found within the designated areas in these six animals is indicated below each profile.

(C) Flow cytometric analysis of spleen cells stained with FITC-conjugated anti-IgM and PE-conjugated anti-CD45R(B220). The more mature IgM^{+}, IgD^{+} splenic B cells are usually taken to be IgM^{low} and would be contained within area R5.

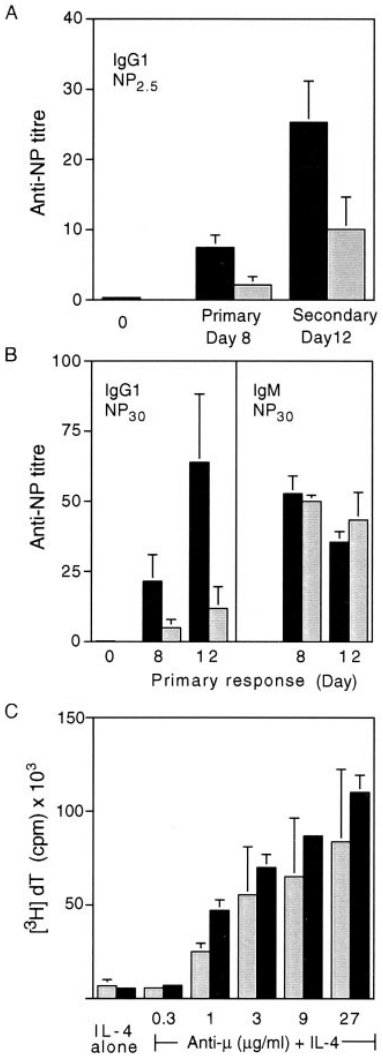

Figure 3. B Cell Responses

(A) Titres of IgG1 anti-NP antibody in the sera of NP-CG immunized mice analyzed by ELISA on $NP_{2.5}$-BSA. The bars (black bars, *Msh2*$^{+/-}$; gray bars, *Msh2*$^{-/-}$) give the mean titres ± SEM (n = 8 for the primary rsponse; n = 4 for the secondary). Titres are given in arbitrary units based on multiplying OD readings in the ELISA by the relevant serum dilution factor.

(B) Titres of IgM and IgG1 anti-NP antibody in the sera of NP-CG immunized mice were analyzed by ELISA on NP_{30}-BSA on the same mice (n = 8) as in (A).

(C) Proliferative responses of splenocytes from *Msh2*$^{+/-}$ (black bars) and *Msh2*$^{-/-}$ mice (gray bars) to IL4 ± F(ab′)$_2$ goat anti-μ were assayed by monitoring incorporation of [^{3}H]thymidine following a 48 hr culture. Each column represents the mean of three mice.

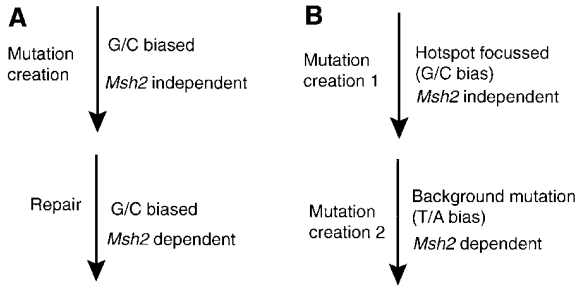

Figure 4. Two Models that Could Account for the Different Pattern of Mutations Observed in MSH2-Deficient and Normal Mice

(A) Hypermutation preferentially creates nucleotide substitutions at G/C residues, but MSH2-dependent mismatch repair also preferentially corrects mismatches at G and C. This is the model put forward by Phung et al. (1998). Additional effects of the *Msh2* disruption would need to be invoked to account for the diminished frequency of mutation that we observe in MSH2-deficient mice.

(B) Mutation creation itself is viewed as a two-stage process. The first stage is MSH2 independent and is strongly biased toward major intrinsic hot spots (which tend to be at G or C). The second stage, triggered by events occurring at the hot spots, introduces new mutations with an A/T bias in other parts of the target by error-prone DNA synthesis. This second stage is dependent on MSH2; in the absence of MSH2, diminished mutation accumulation and increased hot spot focusing would be anticipated.

Hot Spot Targeting

The hypermutation in MSH2-deficient mice shows a greatly increased focusing on the intrinsic hot spots. We do not see how this effect can be readily ascribed to an alteration of extraneous aspects of cellular physiology, but we believe it reflects an effect of the *Msh2* disruption on the mechanics of the process of mutation creation/fixation during hypermutation. Indeed, the results point to there being an *Msh2*-independent phase of mutation targeting that is highly focused on hot spots, with a second, *Msh2*-dependent phase that drives a wider mutation distribution, so redressing the balance of hot spot versus background and G/C versus A mutations.

The nucleotide substitutions created by somatic hypermutation are nonrandomly distributed (Berek and Milstein, 1987). There is a general preference for mutations to be introduced at an RGYW consensus (Rogozin and Kolchanov, 1992) but, over and above this, a number of positions (which usually conform to the RGYW or TA consensus) constitute intrinsic mutational hot spots (Sharpe et al., 1991; Betz et al., 1993; González-Fernández et al., 1994b; Reynaud et al., 1995; Goyenechea and Milstein, 1996; Dörner et al., 1998; Klix et al., 1998; Milstein et al., 1998). The significance of these hot spots is unknown: their local sequence environment could favor nucleotide misincorporation by an error-prone polymerase or allow diminished efficacy of mismatch repair. Alternatively, their location could be highlighting sites at which the hypermutation process is initiated.

Major hot spots are at G/C positions and therefore the increased hot spot targeting that we observe and the bias toward G/C mutation (Jacobs et al., 1998; Phung et al., 1998) discussed by Phung et al. (1998) could, in some sense, be two sides of the same coin. Indeed, the increased mutation at G/C identified by Phung et al. (1998) can in fact be ascribed to greatly increased mutation at the Ser-31 and Ser-77 codons in their *VκOx-1* target gene; these sites are known to be the major intrinsic hot spots of *VκOx-1* (Betz et al., 1993). Equally, however, the increased hot spot focusing that we observe could be a consequence of an overall increase in the G/C bias of the mutational process in MSH2-deficient mice.

Phung et al. propose that the G/C bias of mutations in *Msh2*$^{-/-}$ mice reveals that mutation introduction is highly G/C biased and that MSH2 normally serves a

role in preferentially correcting mismatches at G and C (Figure 4A). Such a model could also account for increased hot spot focusing. Even then, a major implication of our results would still be that mutational targeting at the stage of mutation creation is much more focused on the intrinsic hot spots that has been recognized heretofore.

However, given the finding of hot spot focusing, it is tempting to consider models other than that proposed by Phung et al. (1998). An alternative scenario we propose (Figure 4B) is that mutation creation at hot spots occurs by a mechanism distinct from that applying in the rest of the hypermutation target. For example, nucleotide substitutions could initially be introduced at hot spots and sensed by MSH2, which then, in attempting to repair the hot spot mutations, brings into play an error-prone polymerase that creates mutations outside the hot spots. The distinction between mutations created at either stage is far from precise, except that the first is G/C biased while the second is A biased.

Whatever the mechanism, the analysis of the distribution of mutations in MSH2-deficient mice indicates that there are at least two phases involved in targeting mutation fixation that are sensitive to local DNA sequence. Such a conclusion has also emanated from an analysis of the DNA strand polarity of mutational targeting (Milstein et al., 1998). The first phase is MSH2 independent and highly focused on intrinsic hot spots. The second is MSH2 dependent and allows a wider and differently biased distribution of mutation away from the hot spots—an aspect that is presumably of selective advantage for the adaptive immune response.

Experimental Procedures

Mice

MSH2-deficient mice (de Wind et al., 1995) were kindly provided by Dr. H. te Reile through Dr. K. Brown (CRC Beatson Laboratories, University of Glasgow). *Msh2*$^{-/-}$ males were bred in our barrier unit with females from one of our own lines containing a modified Igκ light chain transgene (M. E. and M. S. N., unpublished data). The mice were genotyped using a PCR-based assay on tail DNA to detect the hygromycin-resistance gene insertion (primers 5′-TGAAA AGCCTGAACTCACC-3′ and 5′-CTGAATTCCCCAATGTCAAG-3′) and to check for exon interruption in *Msh2*. To detect the wild-type exon, primers (5′-CAGGCTACGTAGAGC-3′ and 5′-AACACAAG CATGCCTGGA-3′) were designed around the unique SnaB1 site, which, by comparison with the published human MSH2 germline sequence, lies at the start of exon 12.

Analysis of Mutation

Germinal center [CD45R(B220)$^+$ PNA^{high}] B cells were sorted from Peyer's patches and the J_H4 3′ flanking sequence of endogenous rearrangements of V_HJ558 family members amplified by PCR (consensus V_HJ558 family framework 3 forward primer, 5′-GGAATTCGC CTGACATCTGAGGACTCTGC-3′); J_H-C_H back primer, 5′-GACTAGT CCTCTCCAGTTTCGGCTGAATCC-3′) as described by Jolly et al. (1997) using an Expand High Fidelity PCR System (Boehringer Mannheim) employing six cycles of 93°C (40 s), 64°C–55°C (touch down annealing) (40 s), and 4 min extension times at 72°C followed by a further 30 cycles, but with these extensions performed at 55°C. Amplified DNA was restricted with EcoRI and SpeI, cloned into M13mp19, and sequenced using the −21 M13 primer and Bigdye terminator cycle sequencing (PE Applied Biosystems) in an ABI377 sequencer. Sequences were aligned and analyzed using Pregap and Gap4 software (Bonfield et al., 1995). A 403 bp segment was analyzed for mutations (but excluding the VDJ junction and the 5′-terminal 16 residues of the J_H4 segment). All analysis of hot spots and mutation bias was performed on restricted data after elimination of clonally related sequences identified on the basis of shared VDJ rearrangements. The maximun PCR error for the described conditions was estimated (by sequencing clones from fractionated PNA^{low} B cells) to be less than 0.8×10^{-3}.

Analysis of B Cells and Responses

For immunization, mice (8–12 weeks old) were challenged intraperitoneally with NP_{13}-CG (Solid Phase Sciences, San Rafael, CA) that had been alum precipitated and boosted 24 days later. ELISAs were performed on either NP_{30}-BSA- or $NP_{2.5}$-BSA-coated plates using biotinylated anti-IgM and IgG1 antibodies (Pharmingen) (Herzenberg et al., 1980). Analysis of B cell subpopulations was done using PE-conjugated rat RA3–6B2 monoclonal anti-mouse CD45R(B220) antibody (GIBCO) and fluoresceinated anti-mouse IgM or IgD (Pharmingen); analysis of proliferative responses using $F(ab')_2$ goat anti-mouse μ (Jackson) was performed as previously described (O'Keefe et al., 1996).

Acknowledgments

We thank Caroline Napper for assistance with DNA sequencing and Gareth Williams for carrying out cell proliferation assays. We are grateful to M. Radman for the offer of the MSH2-deficient mice. We acknowledge financial support from the National Foundation for Cancer Research (C.M.), Howard Hughes Medical Institute (M.S.N.), and MRC (M. R. E.). We note that Frey, Weill, and Reynaud (personal communication) have findings analogous to ours with respect to hypermutation in Peyer's patch germinal center B cells from MSH2-deficient mice and that Manser and colleagues (personal communication) have also observed diminished IgG anti-hapten responses in such animals.

Received June 22, 1998.

References

Berek, C., and Milstein, C. (1987). Mutation drift and repertoire shift in the maturation of the immune response. Immunol. Rev. *96*, 23–41.

Betz, A.G., Rada, C., Pannell, R., Milstein, C., and Neuberger, M.S. (1993). Passenger transgenes reveal intrinsic specificity of the antibody hypermutation mechanism: clustering, polarity, and specific hot spots. Proc. Natl. Acad. Sci. USA *90*, 2385–2388.

Bonfield, J.K., Smith, K.F., and Staden, R. (1995). A new DNA-sequence assembly program. Nucleic Acids Res. *23*, 4992–4999.

Cascalho, M., Wong, J., Steinberg, C., and Wabl, M. (1998). Mismatch repair co-opted by hypermutation. Science *279*, 1207–1210.

de Wind, N., Dekker, M., Berns, A., Radman, M., and te Riele, H. (1995). Inactivation of the mouse *Msh2* gene results in mismatch repair deficiency, methylation tolerance, hyperrecombination, and predisposition to cancer. Cell *82*, 321–330.

Dörner, T., Foster, S.J., Brezinschek, H.-P., and Lipsky, P.E. (1998). Analysis of the targeting of the hypermutational machinery and the impact of subsequent selection on the distribution of nucleotide changes in human V_HDJ_H rearrangements. Immunol. Rev. *162*, 161–171.

González-Fernández, A., and Milstein, C. (1993). Analysis of somatic hypermutation in mouse Peyer's patches using immunoglobulin kappa light-chain transgenes. Proc. Natl. Acad. Sci. USA *90*, 9862–9866.

González-Fernández, A., Gilmore, D., and Milstein C. (1994a). Age-related decrease in the proportion of germinal center B cells from mouse Peyer's patches is accompanied by an accumulation of somatic mutations in their immunoglobulin genes. Eur. J. Immunol. *24*, 2918–2921.

González-Fernández, A., Gupta, S.K., Pannell, R., Neuberger, M.S., and Milstein, C. (1994b). Somatic mutation of immunoglobulin lambda chains: a segment of the major intron hypermutates as much as the complementarity-determining regions. Proc. Natl. Acad. Sci. USA *91*, 12614–12618.

Goyenechea, B., and Milstein, C. (1996). Modifying the sequence of an immunoglobulin V-gene alters the resulting pattern of hypermutation. Proc. Natl. Acad. Sci. USA *93*, 13979–13984.

Herzenberg, L.A., Black, S.J., Tokuhisa, T., and Herzenberg, L.A. (1980). Memory B cells at successive stages of differentiation. Affinity maturation and the role of IgD receptors. J. Exp. Med. *151*, 1071–1087.

Jacobs, H., Fukita, Y., van der Horst, G., de Boer, J., Weeda, G., Essers, J., de Wind, N., Engelward, B.P., Samson, L., Verbeek, S., et al. (1998). Hypermutation of immunoglobulin genes in memory B cells of DNA repair-deficient mice. J. Exp. Med. *187*, 1735–1743.

Jolly, C.J., Klix, N., and Neuberger, M.S. (1997). Rapid methods for the analysis of immunoglobulin gene hypermutation: application to transgenic and gene targeted mice. Nucleic Acids Res. *25*, 1913–1919.

Klix, N., Jolly, C.J., Davies, S.L., Bruggemann, M., Williams, G.T., and Neuberger, M.S. (1998). Multiple sequences from downstream of the J kappa cluster can combine to recruit somatic hypermutation to a heterologous, upstream mutation domain. Eur. J. Immunol. *28*, 317–326.

Lebecque, S.G., and Gearhart, P.J. (1990). Boundaries of somatic mutation in rearranged immunoglobulin genes: 5′ boundary is near the promoter, and 3′ boundary is approximately 1 kb from V(D)J gene. J. Exp. Med. *172*, 1717–1727.

Milstein, C., Neuberger, M.S., and Staden, R. (1998). Both DNA strands of antibody gene are hypermutation targets. Proc. Natl. Acad. Sci. USA, in press.

O'Keefe, T.L., Williams, G.T., Davies, S.L., and Neuberger, M.S. (1996). Hyperresponsive B cells in CD22-deficient mice. Science *274*, 798–801.

Parham, P., ed. (1998). Somatic Hypermutation of Immunoglobulin Genes. Immunological Reviews, Vol. 162. (Copenhagen, Denmark: Munksgaard).

Phung, Q.H., Winter, D.B., Cranston, A., Tarone, R.E., Bohr, V.A., Fishel, R., and Gearhart, P.J. (1998). Increased hypermutation at G and C nucleotides in immunoglobulin variable genes from mice deficient in the MSH2 mismatch repair protein. J. Exp. Med. *187*, 1745–1751.

Rajewsky, K. (1996). Clonal selection and learning in the antibody system. Nature *381*, 751–758.

Reynaud, C.A., Garcia, C., Hein, W.R., and Weill, J.C. (1995). Hypermutation generating the sheep immunoglobulin repertoire is an antigen-independent process. Cell *80*, 115–125.

Rogozin, I.B., and Kolchanov, N.A. (1992). Somatic hypermutagenesis in immunoglobulin genes. II. Influence of neighbouring base sequences on mutagenesis. Biochim. Biophys. Acta *1171*, 11–18.

Sharpe, M.J., Milstein, C., Jarvis, J.M., and Neuberger, M.S. (1991). Somatic hypermutation of immunoglobulin kappa may depend on sequences 3′ of C kappa and occurs on passenger transgenes. EMBO J. *10*, 2139–2145.

Storb, U. (1996). The molecular basis of somatic hypermutation of immunoglobulin genes. Curr. Opin. Immunol. *8*, 206–214.

Weill, J.C. (ed). (1996). Somatic Hypermutation: Mechanisms and Signals. Semin. Immunol. *8*.

Winter, D.B., Phung, Q.H., Umar, A., Baker, S.M., Tarone, R.E., Tanaka, K., Liskay, R.M., Kunkel, T.A., Bohr, V.A., and Gearhart, P.J. (1998). Altered spectra of hypermutation in antibodies from mice deficient for the DNA mismatch repair protein PMS2. Proc. Natl. Acad. Sci. USA *95*, 6953–6958.